ELSEVIER

Contents lists available at ScienceDirect

Archives of Biochemistry and Biophysics

journal homepage: www.elsevier.com/locate/yabbi



The spatial distribution of thin filament activation influences force development and myosin activity in computational models of muscle contraction

Axel J. Fenwick, Alexander M. Wood, Bertrand C.W. Tanner

Department of Integrative Physiology and Neuroscience, Washington State University, Pullman, WA, 99164, USA

ARTICLE INFO

Keywords: Muscle mechanics Sarcomere structure Thin filaments activation Computational modeling Cross-bridge kinetics

ABSTRACT

Striated muscle contraction is initiated by Ca²⁺ binding to, and activating, thin filament regulatory units (RU) within the sarcomere, which then allows myosin cross-bridges from the opposing thick filament to bind actin and generate force. The amount of overlap between the filaments dictates how many potential cross-bridges are capable of binding, and thus how force is generated by the sarcomere. Myopathies and atrophy can impair muscle function by limiting cross-bridge interactions between the filaments, which can occur when the length of the thin filament is reduced or when RU function is disrupted. To investigate how variations in thin filament length and RU density affect ensemble cross-bridge behavior and force production, we simulated muscle contraction using a spatially explicit computational model of the half-sarcomere. Thin filament RUs were disabled either uniformly from the pointed end of the filament (to model shorter thin filament length) or randomly throughout the length of the half-sarcomere. Both uniform and random RU 'knockout' schemes decreased overall force generation during maximal and submaximal activation. The random knockout scheme also led to decreased calcium sensitivity and cooperativity of the force-pCa relationship. We also found that the rate of force development slowed with the random RU knockout, compared to the uniform RU knockout or conditions of normal RU activation. These findings imply that the relationship between RU density and force production within the sarcomere involves more complex coordination than simply the raw number of RUs available for myosin cross-bridge binding, and that the spatial pattern in which activatable RU are distributed throughout the sarcomere influences the dynamics of force production.

1. Introduction

The actin and myosin cross-bridge (XB) interaction hydrolyzes ATP to generate force and shortening at the molecular level, which underlies skeletal and cardiac muscle contraction [1,2]. Actin and myosin are the primary proteins comprising the thin and thick filaments, respectively, within the sarcomere. Cross-bridge binding is Ca²⁺-regulated via troponin and tropomyosin, which are the regulatory proteins that run along thin filaments in a stoichiometric ratio of seven actins to one troponin and one tropomyosin. This stoichiometric ratio defines the "structural" regulatory unit (RU) that repeats longitudinally along the length of the thin filament [3]. Cross-bridge binding is also regulated via the interdigitating overlap between thin and thick filaments, which dictates the longitudinal proximity of actin and myosin, and can vary as

sarcomere length changes with muscle shortening or lengthening [4,5]. Therefore, the combination of Ca^{2+} -activated RUs and myofilament overlap determines the potential degree of cross-bridge binding that underlies muscle contraction.

Under normal physiological conditions the spatial, biochemical, and chemomechanical aspects of Ca²⁺-regulated cross-bridge binding, as well as thin filament and thick filament length, are tightly controlled. However, many different myofilament proteins can contribute to improper Ca²⁺-regulation along thin filaments and variations in thin filament length, which can be related to aging, atrophy or disuse, dysregulated development, or skeletal and cardiac muscle pathologies [6]. For example, myriad mutations in the genes of troponin or tropomyosin have been shown to compromise thin filament activation, resulting in contractile dysfunction in muscle diseases [6–8]. Nebulin has been

E-mail address: bertrand.tanner@wsu.edu (B.C.W. Tanner).

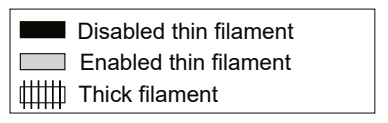
^{*} Corresponding author. 255 VBR, 1815 Ferdinand's Lane, Dept. of Integrative Physiology and Neuroscience, Washington State University, Pullman, WA, 99164-7620. USA.

implicated as a 'molecular ruler' that establishes thin filament length, and mutations in the nebulin gene (NEB) that underlie nemaline myopathy often result in shorter thin filaments and reduced muscle force [9–14]. Shorter thin filaments have also been documented following space flight [15,16], and with atrophy upon muscle injury [17,18]. Tropomodulin and leiomodin can modulate actin polymerization near the free end (pointed end) of thin filaments, thereby altering thin filament length and contributing to skeletal and cardiac muscle disease [13,19–25]. Ca²⁺-activation along thin filaments and the length of thin filaments are two important characteristics of cross-bridge binding and force production within the sarcomere, yet the contributions from each mechanism are difficult to parse experimentally.

Our understanding of striated muscle contraction has benefited from a long history of mathematical and biophysical models of molecular, cellular, and whole-muscle function [1,2,26-33]. Spatially-explicit models of muscle contraction represent a sub-class of these models, which was pioneered by Daniel et al. [34] to investigate the impact of varied filament stiffness on force production between a single pair of thin and thick filaments within the half-sarcomere. Others have expanded upon this idea to examine kinetic properties within the mathematical and biophysical context of a 'digital' sarcomere [35–40]. In this study, we used a half-sarcomere representation comprising multiple thin and thick filaments to modulate the number of thin filament RUs that were capable of being Ca²⁺-activated to bind with myosin. We investigated how variations in thin filament length and RU density affect ensemble cross-bridge behavior and force production by building upon previously published spatially-explicit, multi-filament models of muscle contraction from our laboratory [35,41,42]. The spatial details related to thin filament regulation and thin filament structure investigated herein intrinsically require a model that describes spatial characteristics of thin filament regulation, along and between the myofilaments. While it may be possible (though difficult) to represent these important details within a model using a system of ordinary differential and/or partial differential equations [43], the majority of differential equation models assume independent activity among the of populations of RU and cross-bridges. This assumption of independence fails to represent the coupled protein activity along and between the myofilaments (spatially, mechanically, and biochemically) that underlies muscle function. Under the mathematical assumptions governing this computational paradigm, our simulation predictions begin to separate characteristics of muscle contraction that follow from compromised Ca²⁺-activation along full-length thin filaments vs. shorter thin filaments.

2. Materials and methods

The computational models used in this work build on a series of spatially-explicit models developed over the past 20 years that simulate muscle contraction within a network of linear springs [34,35,38,44]. In short, the current model represents a half-sarcomere that comprises 4 thick filaments and 8 thin filaments to model Ca²⁺-regulated actomyosin cross-bridge binding and force production (Fig. 1). Periodic boundary conditions along the length of the half-sarcomere remove any cross-sectional edge effects along the longitudinal boundary of the simulation. This effectively wraps the external edges of a rectangular region along the length of a myofibril to enable predictions of muscle contraction from a finite number of filaments that represents a sub-section of myofilament lattice space with simple-lattice structure [41]. Boundary conditions at the ends of the filaments (i.e. the M-band and Z-line) are fixed throughout the duration of each simulation, thereby defining the isometric length of the half-sarcomere. This half-sarcomere models includes a linear elastic element between the free-end of thick filaments and the Z-line to represent titin [41,42]. As further described below, we have now implemented two different "knockout" schemes to modulate the spatial distribution of thin filament RUs that are capable of being Ca²⁺-activated to bind with proximal



Uniform Knockout

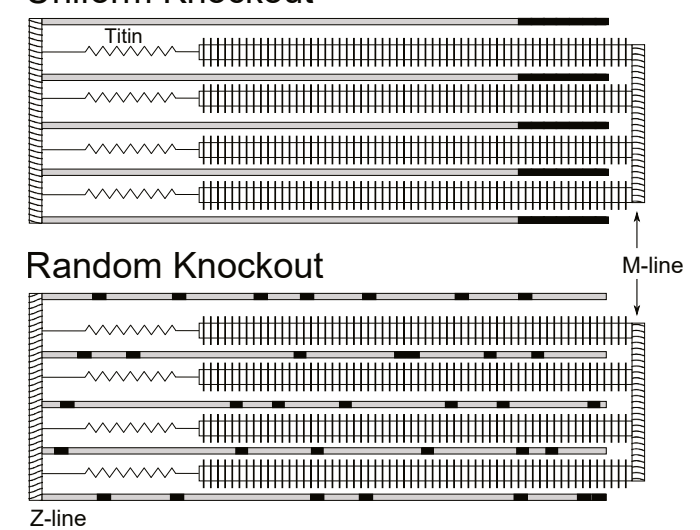


Fig. 1. Model of half-sarcomere organization and thin filament activation "knockout" schemes. Thick filaments conform to normal model geometry, mechanics, and kinetics throughout a simulation. Thin filaments conform to normal model geometry and mechanics, but their Ca²⁺-activation kinetics were effectively partitioned into active regions that are available to bind myosin (grey, having the normal kinetic scheme shown in **Fig. 2**) and inactive or disabled regions that are unavailable to bind myosin (black, effectively having no Ca²⁺-activation kinetics or being 'knocked out'). Example distributions of the two thin filament activation "knockout" schemes, i.e. uniform or random, are depicted for a half-sarcomere.

myosin cross-bridges (Fig. 1). The kinetic scheme also includes cooperative activation of thin filaments from neighboring Ca²⁺-activated thin filament RU and neighboring bound cross-bridges (Fig. 2), as previously described [35].

One advantage of this model is the intrinsic ability to assess spatial effects of thin filament activation on cooperative activation of force production within the half-sarcomere. The Ca²⁺-activatable region of each RU is defined, end to end, along the length of thin filaments, making it amenable to "knocking them out" or making regions of the thin filament unable to bind Ca²⁺. Thus, RU effectively become deactivated throughout the duration of a simulation. It is plausible similar simulations could be performed with the spatially-explicit model from the Mijailovich group, although Ca²⁺-regulation in those models occurs via implementing a long-range continuous flexible chain model [45,46]. Other spatially-explicit models have been used to investigate the distribution of longitudinal vs. radial forces throughout the lattice, without implementing a thin filament regulatory scheme [47,48]. Furthermore, others have developed spatially-explicit models focused on investigating mechanosensitive activation specifically of contraction, force-dependent recruitment from the super-relaxed, myosin OFF state into the disordered-relaxed myosin ON state [49]. While there are limitations to the completeness and breadth that can be explored within each of these spatially-explicit models, they have provided insightful predictions about the molecular mechanisms underlying cross-bridge function among a coupled system of motors throughout the myofilament lattice.

2.1. Myofilament mechanics

Thick filament backbones, thin filaments, cross-bridges, and titin are

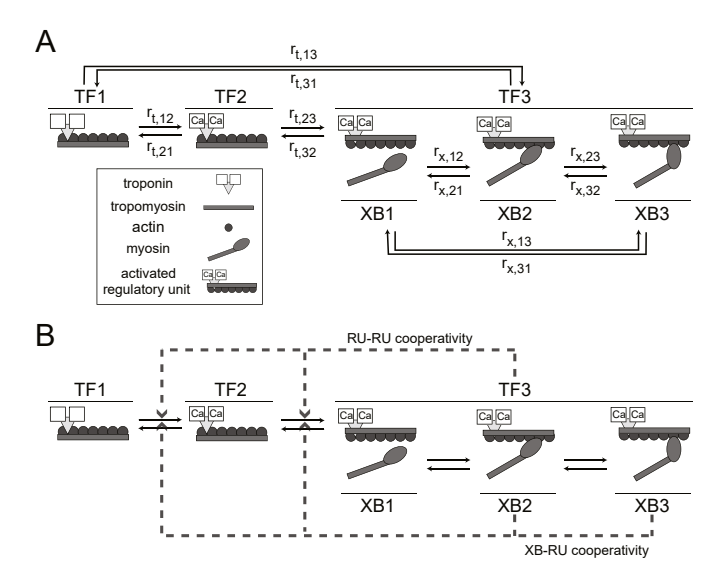


Fig. 2. Model kinetics. The thin filament regulatory units (RU) and thick filament myosin heads have separate, but intertwined, discrete states in the model. (A) The thin filament RU states (TF1-TF3) correspond to whether calcium is not bound to troponin (TF1), calcium is bound to troponin and not available to bind with myosin (TF2), or available to bind myosin (TF3). These states represent thin filament activation behavior for troponin and tropomyosin along thin filaments [35]. If a thin filament RU is in the third state, TF3, it can then be bound by a myosin cross-bridge either weakly (XB2, a pre-power stroke state corresponding to an actin-myosin-ADP-Pi state) or strongly (XB3, a post-power stroke state corresponding to an actin-myosin-ADP state). XB1 represents an unbound cross-bridge state following ATP hydrolysis, corresponding to a myosin-ADP-Pi state. Calcium levels determine RU transition rates, while XB transition rates are determined by the distance between a myosin head and the actin site with which it is binding. (B) Cooperative mechanisms within the model allow for the state of neighboring RUs (i.e. RU-RU cooperativity) and/or neighboring cross-bridges (i.e. XB-RU cooperativity) to augment the probability of thin filament activation. These cooperative pathways are shown as broken arrows originating from a 'source' state (e.g. RU activation or XB binding) to a 'target' the enhanced thin filament transition rate at a neighboring RU (specifically, increasing rates $r_{t,12}$ or $r_{t,23}$ depending upon RU state) [35].

represented as linear springs, such that motion, forces, and deformation within the myofilament network occur solely along the longitudinal direction of the filaments [34,44]. This assumption permits a linear system of equations to calculate the one-dimensional force balance throughout the half-sarcomere at each time-step (dt = 1 ms). Thick and thin filament spring constants were 6060 and 5230 pN nm⁻¹ for unstrained spring elements of length 14.3 and 12.3 nm, respectively. Half-sarcomere length thick filaments were 860 nm (60 thick filament nodes \times 14.3 nm) and thin filaments were 1110 nm (90 actin nodes \times 12.3 nm). These thick filament and thin filament nodes represent model structures for the myosin crowns along thick filament backbones from which myosin heads extend, and actin sites along the thin filament to which myosin can bind [35]. Along each filament, these nodes are connected via linear springs, as described just above, and it is the location of these nodes that is used to track position, force, activation state, and cross-bridge binding state throughout the half-sarcomere model. When myosin heads bind with actin, they are assigned a cross-bridge spring constant of 3 pN nm⁻¹, which is consistent with estimates of cross-bridge stiffness from cellular experiments [50-52]. Sarcomere length was fixed at 2.3 μm (=half-sarcomere length of 1150 nm), representing almost complete thick-to-thin filament overlap (\sim 820 nm) near the plateau of the length-tension relationship [53]. The elastic link representing titin was assigned a spring constant of 0.1344 pN nm⁻¹, and an unstrained, rest-length value of 342 nm. These values provided relaxed (passive) force values of roughly 50 pN, though all force data reported herein are Ca²⁺-activated force values (i.e. total force minus passive force).

2.2. Kinetics

Monte Carlo algorithms drive kinetic state transitions for thin filament activation and cross-bridge binding and cycling (Fig. 2). These effectively consist of a 3-state, discrete time Markov chain for each RU, actin-binding site, and myosin cross-bridge at every time step of the simulation. Specifically, a random number (n) is drawn from a uniform distribution over the open interval (0,1). Any single transition probability (p_{ij}) from state i to state j depends upon the transition rate (r_{ij}) and time-step: $p_{ij} = r_{ij}dt$. Transition probabilities dictate whether there is a forward transition, reverse transition, or no transition:

forward transition
$$= 0 < n < p_{ij}$$
, reverse transition $= p_{ij} < n < p_{ij} + p_{ji}$, no transition $= p_{ii} + p_{ij} < n < 1$.

The rate constants and cooperative kinetics scheme used in these simulations is the same as listed in Table- 3 of Tanner et al., 2012 [35].

Thin filament activation represents three states (Fig. 2A): no Ca²⁺bound to troponin (unavailable to bind myosin), Ca²⁺-bound to troponin (unavailable to bind myosin), and movement of tropomyosin to expose actin-target sites along thin filaments (available to bind myosin). Crossbridge cycling represents three states: XB1 (an unbound cross-bridge state following ATP hydrolysis); XB2 (a weakly bound pre-power stroke state corresponding to an actin-myosin-ADP-Pi state); and XB3 (a strongly bound post-power stroke state corresponding to an actinmyosin-ADP state). However, the actual force generated by a crossbridge depends upon the distance between thick and thin filament nodes and the strain borne by the cross-bridge spring element. As previously described, the cross-bridge transition rates are dependent on position differences between a particular pair of actin and myosin nodes supporting a bound XB [35,44]. For each bound cross-bridge, force borne depends upon the stiffness and distortion of the head from rest-length in the unbound state (xb₀ \approx 5 nm), which includes position differences between the myosin node (where the neck of the XB would extend from backbone = x_m), actin node (or binding site = x_a), and the power stroke state. For XB2 cross-bridge force becomes $k_{xb}((x_a-x_m)-xb_0))$. Energy stored in the cross-bridge is transmitted into the filament lattice with the chemomechanical power stroke transition, and XB3 represents a higher-force state: $k_{xb}(x_a-x_m)$.

All simulations were built upon a cooperative thin filament activation scheme, as previously described [35], which represents cooperative activation mechanisms stemming from RU-RU and XB-RU between neighboring activated RU and bound cross-bridges (Fig. 2B). In brief, the RU-RU cooperative activation pathway stems from a neighboring activated RU that is directly adjacent to the RU undergoing a potential kinetic state transition, occupying the activated state (TF3). If this neighboring RU occupies TF3, then the probability of thin filament activation increases for the RU in question by increasing the rate constant $r_{t,12}$ or $r_{t,23}$ (depending upon which state the RU occupies). Similarly, the XB-RU cooperative activation pathway stems from neighboring cross-bridges occupying the XB2 or XB3 state, which then increases the probability of thin filament activation for the RU in question via increasing the rate constant $r_{t,12}$ or $r_{t,23}$. These rate increases effectively coordinate the strength of cooperative thin filament activation response, which was optimized to represent isometric force-pCa $(pCa = -log_{10}[Ca^{2+}])$ responses measured in rabbit psoas fibers. This model formulation was created to resemble or represent many of the cooperative activation pathways from neighboring activated RU, and weakly or strongly bound cross-bridges, as outlined via the blocked-open-closed model from McKillop and Geeves [26].

With these optimized cooperative kinetics in play, the functional RU activation span becomes \sim 50 nm for all simulations, thereby allowing for the possibility of activating the equivalent thin filament length of \sim 9

actin monomers (or 3 thin filament nodes along one actin helix) upon ${\rm Ca}^{2+}$ -binding to troponin and tropomyosin movement into state TF3 [3, 54]. Given that thin filaments are 1100 nm long, and each troponin complex sits every 37.3 nm along each of the two actin helices that comprise a thin filament, there are 30 structural RU along each helix. This in total leads to 60 RU along each filament, and with the RU activation span of ~50 nm, the functional effects of RU activation are slightly greater than the 37 nm of a structural regulatory unit. Also consistent with prior models, simulations used position-dependent cross-bridge rate transitions as described previously [35,44]. These position dependent rate constants determine how far a cross-bridge can extend to bind with actin, and also underlie how a cross-bridges moves and generates force as it goes through its cross-bridge cycle. This position dependence dictates the chemomechanical state transitions of the cross-bridge, modeled as a linear elastic spring.

2.3. Thin filament RU 'knockout' schemes

Thin filament RU were disabled throughout the half-sarcomere in two ways: uniformly and randomly. Uniform deactivation of RUs (or the uniform RU 'knockout' scheme) was carried out from the free end of the thin filament, mimicking a reduction in thin filament length (Fig. 1). Even with this reduction in activatable regulatory units there were no other changes to the spatial or kinetic parameters underlying thin filament activation and cross-bridge binding with the remaining functional length of thin filaments. Random deactivation (or the random RU 'knockout' scheme) was carried out by randomly deactivating individual RUs along the thin filament. Deactivated RUs were unavailable for Ca²⁺binding, and therefore could not be activated. Deactivation only affected the thin filament kinetics of the model, so thin filament stiffness was not altered by deactivation and any mechanical contributions to the distribution of forces throughout the half-sarcomere were maintained. Under both schemes for disabling RUs, all forms of cooperative activation remained within the model, even though Ca²⁺-activation and crossbridge binding was eliminated for certain thin filament nodes.

2.4. Data analysis

Identical to prior analysis [35,42,44], steady-state data were gathered from each run by calculating the mean of the final 10% of the simulation for each metric. As illustrated in Fig. 3C, it is clear that the simulations reach steady state for the maximal activation level of pCa 4.0. However, the lower [Ca²⁺] require more time to reach steady state, as there is less cross-bridge binding and cycling taking place at these sub-maximal pCa levels. Thus, we employ a graduated scheme to optimize the length of each simulation and the number of runs (i.e. technical replicates) performed at each pCa value. From this we average the final 10% of each individual run (N_{runs}) at a single pCa, for a timespan 0 to t_{max} (Table 1). Consistent with our previous computational studies, the set of steady-state averages at each pCa (gathered from the last 10% of each run) are generated using no fewer than 6400 time steps (6400 > $N_{runs} \times 0.1 t_{max}$). This leads to a set of steady-state values for each individual run at each pCa, from which averages and standard errors are calculated for each metric at each pCa value, and from which statistical analysis can be performed.

ATP utilization was recorded at each time step as the number of cross-bridges that transitioned throughout the 'forward cross-bridge cycle' from the bound, high-force bearing state to the detached state. Consistently, we also count these as unique, completed cross-bridge events during the final 10% of each run to calculate the average myosin cross-bridge attachment duration for each run [41].

Statistical differences were assessed via one-way ANOVA followed by a Tukey-Kramer multiple comparison of the means (p < 0.01). All simulations and analysis were performed using custom algorithms written in MATLAB (The MathWorks, Natick, MA). In the case of parameter estimates for the 3-parameter Hill fits to force-pCa

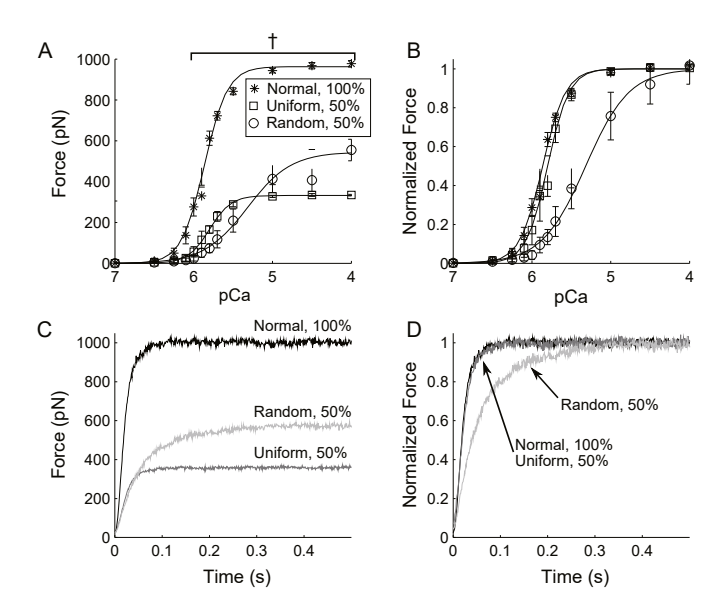


Fig. 3. Steady-state and dynamic force generation as thin filament activation varied. Data are shown for normal thin filament activation (100% functional RUs), 50% random thin filament RU knockout, and 50% uniform thin filament RU knockout. Steady state force is plotted against calcium (mean \pm SE, where pCa = -Log₁₀[Ca²⁺]) for Ca²⁺-activated force values (A) and force values normalized to pCa 4.0 within each data set (B). Daggers denote a significant difference between all groups at a single pCa level (p < 0.01). Average force transients at pCa 4.0 are plotted against time (C), and these values were also normalized to the average steady-state value at pCa 4.0 within each data set (D).

Table 1Duration and number of technical replicates for each simulation as pCa varied.

pCa	N_{Runs}	Duration (s)
≥5.5	11	6
5.0	16	4
≤4.5	32	2

For conditions of pCa 5.5 and greater, simulations were performed for 6 s with 11 technical replicates. Simulations at pCa 5.0 were performed for 4 s with 16 technical replicates. For pCa 4.5 and less, simulations were performed for 2 s with 32 technical replicates.

relationships (Table 2), we used nonlinear least-squares regression to estimate fit parameters and their 99% confidence intervals to identify significant differences between parameter values from different simulations. With a three parameter Hill fit, Max_{fit} represents the maximal, asymptotic, steady-state force predicted by the model; pCa₅₀ defines the pCa value at the force level that is half-way between the relaxed force value (pCa 8) and maximal force (pCa 4), which represents Ca^{2+} -sensitivity of force production. The Hill coefficient, n_{H} , is the tangent of the sigmoidal force-pCa curve-fit at the pCa₅₀ value.

Table 2 Characteristics of tension-pCa relationships in simulation in multiple KO regimes (mean \pm SE).

	Normal	50% Uniform KO	50% Random KO
F _{max} (pN)	977 ± 16	334 ± 3.7^a	$555\pm5.3^{\text{a}}$
Max _{fit} (pN)	963 ± 3.0	$332\pm1.7^{\text{a}}$	546 ± 6.9^{a}
pCa ₅₀	5.86 ± 0.003	5.80 ± 0.005	5.32 ± 0.021^{a}
n_H	2.97 ± 0.059	3.18 ± 0.103^{a}	1.57 ± 0.077^{a}

 F_{max} , steady-state force value at pCa 4.0.

 Max_{fit} , pCa₅₀, and n_H represent fit parameters to a 3-parameter Hill equation for Max_{fit}

the steady-state force (F_{ss}) vs. pCa relationship: $F_{ss}(pCa) = \frac{MaC_{H}t}{1 + 10^{n_H(pCa - pCa_{50})}}$.

a Different from normal based on a 99% confidence interval.

3. Results

3.1. Force development as Ca²⁺-activation varied

Steady-state force production and temporal dynamics of force production are shown in Fig. 3 for simulations with normal thin filament activation (100% functional RUs), 50% random thin filament RU knockout, and 50% uniform thin filament RU knockout. As [Ca²⁺] increased, steady-state force production increased as well, following the expected sigmoidal relationship for all conditions. These force-pCa relationships were fit to a three-parameter Hill equation to assess the effects of random vs. uniform reductions in thin filament activation on calcium sensitivity and cooperativity of force production (Table 2). Reducing the number of functional thin filament RUs by 50% decreased maximal steady-state force by 43.19 \pm 0.54% for the random reduction and 65.81 \pm 0.38% for the uniform reduction, compared to the normal condition (Fig. 3A). The 50% random reduction diminished Ca²⁺sensitivity of force (by 0.54 pCa units) and the 50% uniform reduction only modestly decreased Ca²⁺-sensitivity of force (by 0.06 pCa units), compared to the normal condition. The 50% random reduction also diminished cooperative force development, shown by the ~50% reduction in the Hill coefficient (n_H) compared to the normal condition. The 50% uniform reduction did not affect cooperative force development compared to the normal condition, with $n_{H} \approx 3$ for both conditions. These differences can be observed most clearly by normalizing the three steady-state force-pCa relationships to their maximal steady-state force value (Fig. 3B). Comparable experiments in rabbit psoas fibers showed that randomly reducing about 50% of the Ca²⁺-activatable troponin C along thin filaments also reduced maximal force by \sim 40–50%, reduced Ca²⁺-sensitivity by \sim 0.35 pCa units, and reduced n_H by ~ 1.5 [54], all of which agree with our simulation predictions using the random RU knockout scheme. We were somewhat surprised to see such similarities between the normal simulations (i.e. 100% functional RU) and the simulation results with the 50% uniform reduction, which implies that the cooperative activation pathways underling force development were largely preserved in simulations where thin filament activation was uniformly knocked out from the free end of thin filaments. In contrast, random reductions in thin filament RU activation compromised cooperative activation along thin filaments and more greatly disrupted Ca2+-activated force development, compared to the random reduction in filament length.

3.2. Rates of force development

Time-series traces for the force development transients at maximal activation (pCa = 4.0) are shown in Fig. 3C. Normalizing these data to maximal force within each condition revealed that the random knockout significantly slowed the rate of force development (k_{dev}) at maximal activation (Fig. 3D). The dynamics of force production were only slightly slower than normal with the uniform reduction in thin filament RU activation (Figs. 3D and 4). At maximal Ca²⁺-activation the rates of force development were similar for the normal and 50% uniform reduction in thin filament activation but slowed for the 50% random reduction in thin filament activation. Similar findings persisted at Ca²⁺-activation levels between pCa 5.0 and 4.0 (Fig. 4). Comparable experimental findings to evaluate these kinetic predictions remain limited, as the rabbit psoas fiber study where Ca²⁺-activatable RUs were randomly reduced did not report any kinetics measurements [54]. Data from a similar study using rat trabeculae (and reconstituting thin filaments with a mixture of 50% ${\rm Ca}^{2+}$ -activatable troponin and 50% non-activatable troponins) showed slower rates of tension redevelopment (i.e. k_{TR} measurements) at sub-maximal pCa levels but not at maximal activation, compared to normal conditions [55]. Therefore, our predictions that randomly reducing RU slows force development at sub-maximal pCa levels are consistent with these empirical findings, but not at maximal activation. Findings from this later study also suggested that

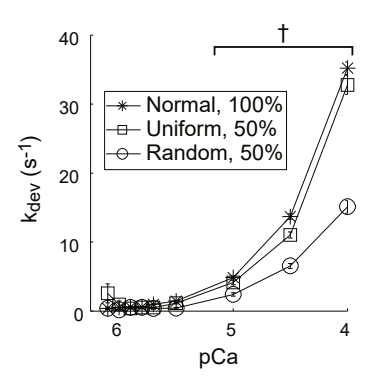


Fig. 4. Rates of force production (k_{dev}) as thin filament activation varied. Data are shown for normal thin filament activation (100% functional RU), 50% random thin filament RU knockout, and 50% uniform thin filament RU knockout. k_{dev} values are plotted against calcium, calculated from the simulation time required to reach 50% of steady-state force (mean \pm SE). Daggers denote a significant difference between all groups at a single pCa level (p < 0.01).

the functional RU span may be shorter in cardiac muscle (spanning ${\sim}4$ actins) [55] than in skeletal muscle (spanning ${\sim}9{\text -}11$ actins) [54]; a structural regulatory unit spans 7 actins. It is plausible these differences in RU activation span between muscle types could also influence k_{TR} measurements differently as pCa and/or the number of activatable RU varies. In combination, our kinetic predictions again suggest that cooperative mechanisms of force production were largely preserved with uniform reductions in thin filament activation, but cooperative activation is compromised for random reductions in thin filament RU activation (Figs. 3–4).

3.3. Graduated reductions in RU density

Steady-state characteristics of contractility, thin filament activation, and cross-bridge activity are shown for maximal Ca²⁺-activation (pCa = 4.0, Fig. 5) and sub-maximal Ca^{2+} -activation (pCa = 5.8, Fig. 6) as activatable RU density decreased. First, we describe these responses at pCa 4.0 and then for pCa 5.8. As shown in Fig. 3, decreasing RU density resulted in an expected decrease in force, but this decrease did not follow a 1:1 linear relationship to the fractional RU density shown by the dashed line in Fig. 5A. Random RU reduction resulted in smaller force decreases than anticipated by a 1:1 decrease in the number of Ca²⁺activatable RU, with force remaining greater than 1:1 across the range of fractional RU densities that were simulated. These findings are consistent with experimental findings from the rabbit psoas fiber study where Ca²⁺-activatable RUs were randomly reduced, which also showed that force remained greater than the 1:1 relationship for fractional RU density values greater than 20% [54]. In contrast, the uniform RU reduction resulted in larger force decreases than random RU reduction, with force values remaining near the 1:1 relationship for fractional RU densities above 70%, and falling below the 1:1 relationship at fractional RU densities of 50% and 60%. The number of bound cross-bridges followed the same relationship as maximal force, indicating that the force decreases stem from reduced cross-bridge binding (Fig. 5B), and not reduced force per bound cross-bridge.

The proportion of thin filament sites that are activated by the binding of Ca^{2+} is shown in Fig. 5C (normalized to the number of sites that are activated during maximal activation of the normal thin filament, i.e. 100% of the RUs). While each point along the x-axis represents the same number of available RUs between the random and uniform knockout schemes, more of the thin filament was activated with random RU reductions than uniform RU reductions of the same magnitude. However, the possible number of RUs that can be Ca^{2+} -activated also changes as the number of activatable RUs were reduced. Thus, thin filament

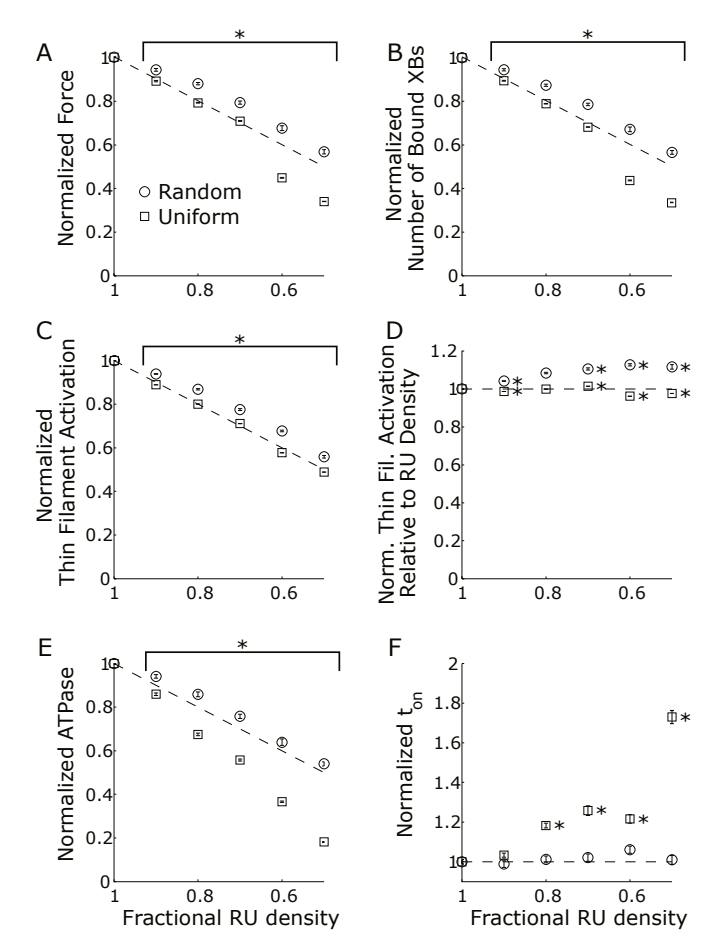


Fig. 5. Random vs. uniform "knockout" of thin filament RU activation at pCa 4. Values of A) force, B) cross-bridge binding, C) Ca^{2+} -activated RUs, D) Ca^{2+} -activated RUs scaled to account for "knockout" within each simulation, E) ATPase activity, and F) myosin attachment time (t_{on}) are plotted against activatable RU density. All data are normalized to the normal thin filament activation value (100% functional RU; mean \pm SE). Asterisks (*) denote values that are different from the normal, 100% functional RU value (p < 0.01). The dashed lines indicate a 1:1 decrease in fractional RU density (A, B, C, E), or unity (D, F).

activation values were also normalized to the relative density of RUs that were capable of being Ca^{2+} -activated within a simulation. This second normalization shows that the relative amount of thin filament activation slightly increases as RUs are randomly knocked out, and that relative thin filament activation levels remain near unity as RUs were uniformly knocked out from the free end of thin filaments, for most simulations (Fig. 3D). However, at 50% and 60% fractional RU density, normalized thin filament activation levels fall slightly below this unity line with the uniform RU reductions (Fig. 3D). These data suggest that there may be coupled effects of thin filament activation pattern along the filament that underlie the predicted levels of force production discussed just above (Fig. 5A), which differ between two RU knockout schemes.

Cross-bridge ATP utilization can be calculated from the simulations via tracking the binding and unbinding of cycling cross-bridges that hydrolyze a single ATP molecule. Random RU reduction resulted in slightly increased ATPase activity (compared to a hypothetical 1:1 decrease), while uniform RU reduction significantly decreased ATPase activity (Fig. 5E). In both cases, the decreased ATPase activity can be primarily attributed to the decrease in cross-bridge binding (Fig. 5B). However, calculations of cross-bridge attachment time (t_{on}) show that t_{on} does not change much with random RU reductions and that cross-bridges remain bound for longer duration with uniform RU reductions

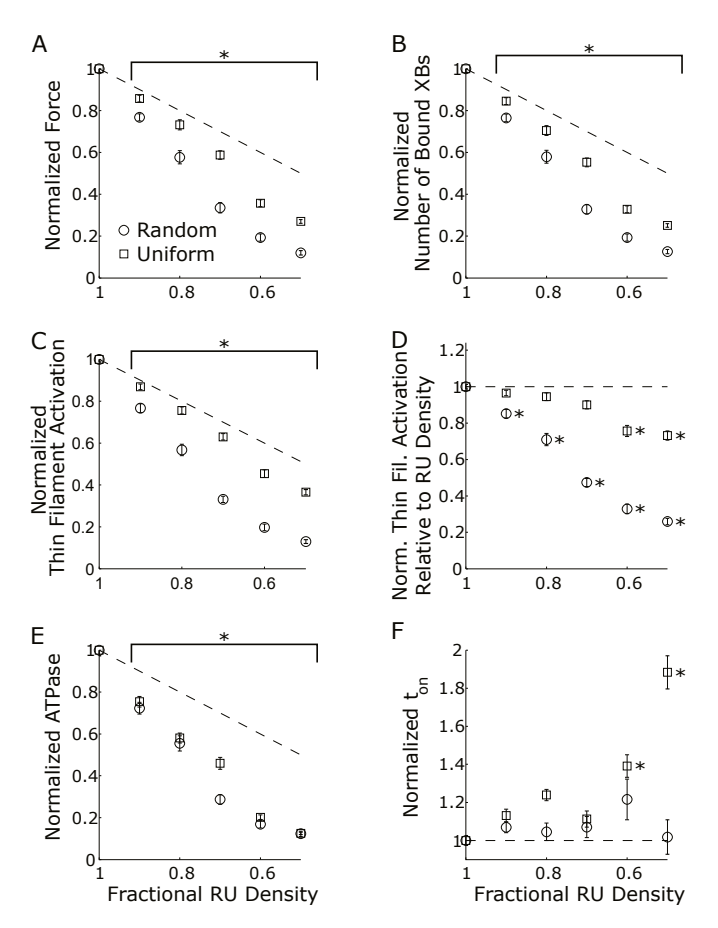


Fig. 6. Random vs. uniform "knockout" in thin filament RU activation at pCa 5.8. Values of A) force, B) cross-bridge binding, C) Ca^{2+} -activated RUs, D) Ca^{2+} -activated RUs scaled to account for "knockout" within each simulation, E) ATPase activity, and F) myosin attachment time (t_{on}) are plotted against activatable RU density. All data are normalized to the normal thin filament activation value (100% functional RU; mean \pm SE). Asterisks (*) denote values that are different from the normal, 100% functional RU value (p < 0.01). The dashed lines indicate a 1:1 decrease in fractional RU density (A, B, C, E), or unity (D, F).

(Fig. 5F). Thus, cross-bridge activity was not greatly affected by random reductions in RU density. In contrast, uniform reductions in RU density increased attachment time and slowed the overall rate of cross-bridge cycling, thereby reducing ATPase activity and force development.

Given that *in vivo* intracellular calcium levels are sub-maximal [56], we were interested to explore how simulation predictions for both RU knockout schemes differ from those presented at maximal activation (Fig. 5). At sub-maximal Ca²⁺-activation levels near the pCa₅₀ value of the force-pCa relationship under normal RU conditions (pCa 5.8), decreasing RU density resulted in an expected decrease in force (Fig. 6A). Random RU reduction significantly decreased force production, below the 1:1 relationship, which shows greater decreases in force production as Ca²⁺-activatable RU density decreased at sub-maximal pCa than comparable simulations at pCa 4.0. In contrast, the uniform RU reduction at pCa 5.8 (Fig. 6A) produced similar trends to those observed at pCa 4.0 (Fig. 5A). Again, simulations predicted well-matched responses between force and the number of bound cross-bridges for both RU knockout schemes at pCa 5.8 (Fig. 6B), as were our findings at pCa 4.0.

At pCa 5.8, the random RU reduction and uniform RU reduction resulted in less thin filament activation than either comparable RU knockout scheme at pCa 4.0. At pCa 5.8, the thin filament activation fell below the 1:1 relationship for both RU knockout schemes as functional RU decreased (Fig. 6C–D), whereas thin filament activation was greater

than the 1:1 relationship for random reductions and near the 1:1 relationship for uniform reductions at pCa 4.0. Consistent with the decrease in cross-bridge binding at pCa 5.8 vs. 4.0, ATPase activity also decreased as RU density was reduced for both knockout conditions (Fig. 6E), compared to pCa 4.0. However, the change in ton was relatively flat with random RU reduction and ton increased non-linearly with uniform RU reduction at submaximal pCa (Fig. 6F), which is similar to the prediction at pCa 4.0 (Fig. 5F), suggesting that the large decreases in ATPase at pCa 5.8 primarily stem from decreases in the number of bound cross-bridges rather than altered kinetics for which bound cross-bridges go through the cross-bridge cycle.

4. Discussion

The purpose of these computational simulations was to examine how the loss of activatable RUs along the thin filament impacts dynamics of force generation and cross-bridge binding within a sarcomere. This loss was modeled as either a uniform disabling of RUs from the pointed end of the thin filament (equivalent to a reduction in thin filament length) or as a random disabling of RUs throughout the thin filament. In summary, we find that force decreased with a uniform loss of RUs, but the normalized force-pCa relationship and dynamics of force production were not very different than we observed for normal conditions. Force also decreased with the random loss of RU activation, but calcium sensitivity of the force-pCa relationship was reduced and the rates of force production slowed in comparison to normal conditions. Throughout the Results section presented above we made comparisons between our simulation results from the random RU reductions with similar experiments using skinned rabbit psoas and rat cardiac muscle fibers [54,55]. In general, our predictions were largely consistent with these previous experimental results where the number of Ca²⁺-activatable RU along thin filaments were reduced (Figs. 3A, 4 and 5A). On the other hand, comparable experimental studies demonstrating the effects of uniform reductions in RU activation or shortening thin filament length are limited. A portion of the viable comparisons for shortened thin filament length are further discussed below, primarily related to findings from nebulin knockout mice [57] or investigations of nemaline myopathies [58].

4.1. Implications underlying uniform reductions in activatable RU

The degree of overlap between the thick and thin filaments is a primary determinant of force within a sarcomere; more overlap increases the availability of actin along thin filament to which crossbridges can bind and generate force [53]. Accordingly, a decrease in the length of either filament would effectively decrease overlap and subsequently decrease Ca²⁺-activated force. However, the length of the thick filament does not vary significantly in vertebrates, and is fixed around 1.6 µm [59,60]. In contrast, thin filament length does vary and depends on the species and muscle type. Even in healthy human muscle the thin filament varies between 1.1 and 1.3 µm, and modulating this length shifts characteristics of the force-length relationship [61-64]. Our simulations suggest that these changes in the force-length relationship likely follow from decreases in cross-bridge binding and filament overlap, but the dynamics of force production and cross-bridge activity are unlikely to greatly affect the force length response over this 0.2 µm change in thin filament length.

During myogenesis, nebulin assists in the initial assembly of I- and Z-bands to set the pattern and spacing of the sarcomeres constituting a myofibril [10]. When nebulin is knocked down in skeletal tissue, thin filament length becomes more heterogeneous and decreases on average, resulting in lower muscle force production [11,57,65,66]. Mutations in the nebulin gene *NEB* are the most common cause of nemaline myopathy 2 (NEM2) [58,67]. Analogous to nebulin knock down in animal models of NEM2, patients with NEM2 mutations have shorter and more variable thin filament lengths [58]. With a smaller overlap region, fewer

cross-bridges are able to bind and less force is produced for a given activation level, especially at longer sarcomere lengths. Additionally, loss of uniform filament length throughout a fiber means that there can no longer be an optimal overlap length, or that it is less consistent and reproducible from muscle to muscle (or person to person), as the plateau of a sarcomere length-force curve becomes less well-defined [6,12]. Mutations in nebulin may also disrupt the binding interactions with actin and/or tropomyosin/troponin complexes, resulting in deficits in cross-bridge cycling and calcium activation [58,68,69].

When we uniformly disabled RUs from the end of the thin filament, we observed decreased force during both maximal activation (pCa = 4.0; Figs. 3 and 5A) and during submaximal activation (pCa = 5.8; Figs. 3 and 6A). The loss of RUs reduces the number of available myosin binding sites on the thin filament, and therefore less overall force is produced in the sarcomere. This finding is consistent with studies which measured decreased force in muscles from nebulin knockout mice, which was attributed in part to decreased thin filament length [57,66]. When we disabled 0-30% of the thin filament RUs at maximal activation, we observed a negative and mostly linear relationship with force; e. g. disabling 30% of the RUs reduced force by ~30%. However, force dropped more greatly as more RUs were disabled, such that disabling 50% of the filament caused force to drop by \sim 66% (Figs. 3 and 5A). This disproportionate decrease in force was further exacerbated during submaximal calcium activation (Fig. 6A). Therefore, reducing thin filament availability has a more complicated effect on force production than simply changing the number of potential actin-myosin cross-bridge interactions due to thin filament overlap.

In the uniform RU knockout simulations performed here and in experiments involving nebulin knockout in mice [57,66], force decreases as the overlap between the thick and thin filament is reduced. This idea is not new, and the phenomena is well understood for the role it plays in the force-length relationship, as changing sarcomere length also affects this overlap [70]. However, more mechanical processes are being influenced by increased sarcomere length than simply reduced filament overlap, such as increased calcium-sensitivity, increased passive and active force levels, reduced lattice spacing, and other cellular properties than can change with sarcomere length [70-81]. We did not alter sarcomere length with the current simulations, and our predictions from the uniform reductions in RU activation only partially reflect on the changes in force that occur with varied sarcomere lengths. For instance, we did not investigate how the contributions of passive elements, such as titin, vary with sarcomere length, as the titin PEVK regions may interact with the thin filament during activation in a manner which decreases the effective spring length of titin and therefore may increase titin stiffness to augment passive forces during stretch [82,83]. These compounding factors mean that altering sarcomere length is not a proxy for the study of reduced filament overlap, although future computational models may provide a tractable option to isolate these coupled effects on muscle force associated with dynamic changes in sarcomere length.

4.2. Implications underlying random reductions in activatable RU

The location and distribution of the disabled RUs is also important. If only the number of available RUs determined the mechanics, then we would expect to observe a similar force profile regardless of the activatable RU distribution along the thin filament. When we randomly disabled an equivalent number of RUs for both knockout schemes, we observed a different relationship between force and fractional RU density compared to uniformly disabling RUs from the pointed end of the thin filament. At maximal activation, we observed a nearly linear relationship between force and ${\rm Ca}^{2+}$ -activatable RU density for both knockout schemes, although force was greater than the 1:1 relationship (dashed line Fig. 5A) with the random RU reduction and force was at, or below, the 1:1 relationship with the uniform RU reduction. These different trends may follow from the activatable RU occupying the ${\rm Ca}^{2+}$ -

activated state (TF3, Fig. 2A) at maximal activation. Any uniform decreases in RU activation remove a length of the thin filament, but with random reductions in RU activation there remains a small section at the overlap region between neighboring RUs that can bind cross-bridges (i. e. near the edge of a remaining Ca²⁺-activatable RU). Thus, random reductions in RU density led to a larger fraction of the thin filament that can bind available cross-bridges binding, albeit discontinuous Ca²⁺activated portions of the thin filament, compared to similar decreases the number of activatable RU with the uniform knockout scheme (even though the remaining length of the thin filament is completely activated and contiguous with the uniform RU knockout). This interpretation would be consistent with estimates from a psoas muscle fiber study that suggested Ca²⁺-binding to troponin activates a portion of the thin filament slightly greater than the 37 nm (or 7 actins) associated with a structural regulatory unit [54]. Consistently, this may follow from our model dictating a functional RU activation span of roughly 50 nm (or roughly 9 actins) when RUs occupy state TF3. Our prior simulations have also shown that reducing the activation span to 37 nm may compromise the cooperative force response and reduce the value of the Hill coefficient of the force-pCa [35]. In addition, cooperativity of the force-pCa relationship was significantly lower when RUs were randomly disabled ($n_H \approx 1.5$) compared to either the uniform RU reductions ($n_H \approx$ 3.2) or normal conditions ($n_H \approx 3.0$, Table 2). Together, these data suggest that random RU reductions disrupt mechanisms of cooperative activation between neighboring RU more than comparable RU reductions with the uniform knockout scheme, where neighboring RU interactions are completely preserved even though a larger, contiguous portion of the thin filament becomes unable to bind cross-bridges.

The kinetics of force production also depended upon the way that RUs were disabled along thin filaments. The rate of force development was significantly slower when RUs were randomly disabled, but the rate of force development was relatively unchanged (compared to normal) when RUs were uniformly disabled (Figs. 3D and 4). However, it is unclear if slower force development directly followed from changes in cooperative activation or other cross-bridge properties. Previous studies attempting to limit the number of neighboring RU interactions have shown minimal or no dependency of the rate of force development on thin filament cooperativity [55,84-86]. To this end, we also observed little change in the average cross-bridge attachment time with the random RU reductions, suggesting that the slower force development was not due to changes in cross-bridge cycling rates. Therefore, the slower force development likely follows from reduced overall cross-bridge binding and the subsequent inability to maintain thin filament activation between multiple, adjacent RUs, thereby slowing the force development throughout the sarcomere and prolonging the time to reach steady-state force levels [87].

The thin filament integrates multiple cooperative mechanisms which increase force production non-linearly with increased Ca²⁺ activation. These mechanisms include cooperative Ca²⁺ binding to troponin-C, stabilization of RU activation following strong cross-bridge binding, and interactions between neighboring RU units [3,32,88]. Ca²⁺ activation of the troponin complex induces allosteric movement of tropomyosin to reveal potential myosin binding sites on the thin filament. This transition of the RU from an 'off' to an 'on' state is stabilized following the formation of strong myosin cross-bridges, which increases the likelihood of further cross-bridge biding within the same RU, or promote activation of neighboring RUs as well. Additionally, tropomyosin backbones lay along the length of the thin filament with an overlap of 5-10 residues which allows for end-to-end interactions between adjacent RUs that can increase their propensity to switch to an 'on' state as well [88,89]. It is the later of these mechanisms, RU-RU cooperativity, which is diminished when RUs are disabled. Theoretically, we would eliminate RU-RU cooperativity along the thin filament if we disabled every other RU (50%), and conversely disabling the same number of RUs as a uniform, cohesive block would not affect RU-RU cooperativity throughout the remainder of the filament (save for the single RU where

the disabled and non-disabled regions meet). In these simulations, we randomly disabled RUs, so each unit had between 0 and 2 available neighbors to interact with, which resulted in decreased, but not abolished, cooperativity (Fig. 3B). Altogether, findings from these computational simulations help illustrate the relationship between thin filament activation and cooperative mechanisms therein that underlie force development, which are highly dependent on the location and spacing of the activatable RUs throughout the sarcomere.

4.3. Model limitations and future directions

As with any computational model, the model represents a detailed hypothesis formulated from a finite number of parameters to represent one's understanding of how a system works and from which the model can be used to investigate or test a finite set of questions. Computational modeling helps illustrate fundamental relationships within the system, some of which can be validated experimentally, and all predictions are tied to the basic assumptions of each model formulation. The spatiallyexplicit, multi-filament computational model of muscle contraction used herein has been formulated to investigate mechanisms underlying cooperative activation of contraction, some of which are difficult or impossible to investigate experimentally (such as changes in crossbridge or filament stiffness, or isolating different pathways for RU-RU activation vs. XB-RU activation). However, there are limitations to this current model formulation that may be lacking and could influence the interpretation of our findings. For example, this model does not include mechanical or regulatory aspects of myosin binding protein-C, a thickfilament regulatory protein that is known to augment thick-filament stiffness [90], which may increase thin filament activation in the C-zone of the sarcomere [91], and can slow cross-bridge kinetics [92]. Although our cross-bridge kinetics scheme (Fig. 2) leads to rate transitions being affected by the RU activation levels, and forces and motions generated by neighboring cross-bridges along the thick (and thin) filaments, the current kinetic scheme does not involve a mechanosensitive myosin OFF-ON transition (i.e. super-relaxed state transition into the disordered relaxed state) based on the force profile along the length of the thick filament [74,93,94]. Over the past decade this mechanosensitive thick filament OFF-ON regulatory pathway is becoming better understood, and the implications for dynamic regulatory coupling between the thick and thin filaments could represent a renaissance for the way physiologist and biophysicist think about muscle regulation dynamics. Additionally, our current model does not account for the distribution of longitudinal vs. radial forces throughout the myofilament lattice, which may have important implications for muscle efficiency, and energy storage and release within the sarcomere during contraction and relaxation [47,48]. There is also evidence that the stiffness of titin may be Ca²⁺ sensitive, either through E-rich motifs on the PEVK segment or through interactions with the thin filament [82,83,95,96], which could augment passive force levels (and influence active force levels given the additional regulatory mechanisms described just above) as intracellular [Ca²⁺] increases throughout a contraction. While we model the length-dependent passive force contribution of titin, this process is not Ca²⁺ sensitive in our current model. One can envision how these additional mechanisms could be implemented with future spatially-explicit model formulations, and their omission may influence some aspects of our simulations predictions herein. Nonetheless, the focus of this study was to test similarities and differences in the force-pCa response, contractile kinetics, RU activation, and cross-bridge activity as RU were randomly vs. uniformly knocked out along the length of thin filaments. Our data suggest that spatial patterning of thin filament activation plays an important role to augment contractility under normal conditions. When the length of thin filaments are reduced under isolated conditions, with all else being equal, the primary detriment is total force production rather than associated changes in Ca²⁺-sensitivity or rates of force development.

Acknowledgements

Funding: This work was supported by grants from the American Heart Association [19TPA34860008] and National Science Foundation [1656450].

References

- A.F. Huxley, Muscle structure and theories of contraction, Prog. Biophys. Chem. 7 (1957) 255–318.
- [2] A.F. Huxley, R.M. Simmons, Proposed mechanism of force generation in striated muscle, Nature 233 (1971) 533–538, https://doi.org/10.1038/233533a0.
- [3] A.M. Gordon, E.E. Homsher, M. Regnier, Regulation of contraction in striated muscle, Physiol. Rev. 80 (2000) 853–924.
- [4] H.E. Huxley, J. Hanson, Changes in the cross-striations of musle during contraction and stretch and their structural interpretation, Nature 173 (1954) 973–976, https://doi.org/10.1038/173973a0.
- [5] O. Tsukamoto, M. Kitakaze, Biochemical and physiological regulation of cardiac myocyte contraction by cardiac-specific myosin light chain kinase, Circ. J. 77 (2013) 2218–2225, https://doi.org/10.1253/circj.CJ-13-0627.
- [6] J.M. de Winter, B. Joureau, E.J. Lee, B. Kiss, M. Yuen, V.A. Gupta, C.T. Pappas, C. C. Gregorio, G.J.M. Stienen, S. Edvardson, C. Wallgren-Pettersson, V.L. Lehtokari, K. Pelin, E. Malfatti, N.B. Romero, B.G.V. Engelen, N.C. Voermans, S. Donkervoort, C.G. Bönnemann, N.F. Clarke, A.H. Beggs, H. Granzier, C.A.C. Ottenheijm, Mutation-specific effects on thin filament length in thin filament myopathy, Ann. Neurol. 79 (2016) 959–969, https://doi.org/10.1002/ana.24654.
- [7] J.C. Tardiff, Thin filament mutations: developing an integrative approach to a complex disorder, Circ. Res. 108 (2011) 765–782, https://doi.org/10.1161/ CIRCRESAHA.110.224170.
- [8] H. Tajsharghi, Thick and thin filament gene mutations in striated muscle diseases, Int. J. Mol. Sci. 9 (2008) 1259–1275, https://doi.org/10.3390/ijms9071259.
- [9] A.S. McElhinny, C. Schwach, M. Valichnac, S. Mount-Patrick, C.C. Gregorio, Nebulin regulates the assembly and lengths of the thin filaments in striated muscle, J. Cell Biol. 170 (2005) 947–957, https://doi.org/10.1083/jcb.200502158.
- [10] A. McElhinny, Nebulin the nebulous, multifunctional giant of striated muscle, Trends Cardiovasc. Med. 13 (2003) 195–201, https://doi.org/10.1016/S1050-1738(03)00076-8.
- [11] H.L. Granzier, C.A.C. Ottenheijm, New insights into the structural roles of nebulin in skeletal muscle, J. Biomed. Biotechnol. 2010 (2010) 1–7, https://doi.org/ 10.1155/2010/968139.
- [12] C.A.C. Ottenheijm, C.C. Witt, G.J.M. Stienen, S. Labeit, A.H. Beggs, H.L. Granzier, Thin filament length dysregulation contributes to muscle weakness in nemaline myopathy patients with nebulin deficiency, Hum. Mol. Genet. 18 (2009) 2359–2369, https://doi.org/10.1093/hmg/ddp168.
- [13] R. Littlefield, V.M. Fowler, Defining actin filament length in striated muscle: rulers and caps or dynamic stability? Annu. Rev. Cell Dev. Biol. 14 (1998) 487–525, https://doi.org/10.1146/annurev.cellbio.14.1.487.
- [14] M. Kruger, J. Wright, K. Wang, Nebulin as a length regulator of thin filaments of vertebrate skeletal muscles: correlation of thin filament length, nebulin size, and epitope profile, J. Cell Biol. 115 (1991) 97–107, https://doi.org/10.1083/ ich 115.1.97
- [15] D.A. Riley, J.L.W. Bain, J.L. Thompson, R.H. Fitts, J.J. Widrick, S.W. Trappe, T. A. Trappe, D.L. Costill, Decreased thin filament density and length in human atrophic soleus muscle fibers after spaceflight, J. Appl. Physiol. 88 (2000) 567–572, https://doi.org/10.1152/jappl.2000.88.2.567.
- [16] D.A. Riley, J.L.W. Bain, J.L. Thompson, R.H. Fitts, J.J. Widrick, S.W. Trappe, T. A. Trappe, D.L. Costill, Thin filament diversity and physiological properties of fast and slow fiber types in astronaut leg muscles, J. Appl. Physiol. 92 (2002) 817–825, https://doi.org/10.1152/japplphysiol.00717.2001.
- [17] A. Volodin, I. Kosti, A.L. Goldberg, S. Cohen, Myofibril breakdown during atrophy is a delayed response requiring the transcription factor PAX4 and desmin depolymerization, Proc. Natl. Acad. Sci. Unit. States Am. 114 (2017) E1375–E1384, https://doi.org/10.1073/pnas.1612988114.
- [18] D.A. Riley, J.L.W. Bain, J.G. Romatowski, R.H. Fitts, Skeletal muscle fiber atrophy: altered thin filament density changes slow fiber force and shortening velocity, Am. J. Physiol. Cell Physiol. 288 (2005) C360–C365, https://doi.org/10.1152/ aincell_00386_2004
- [19] R.S. Littlefield, V.M. Fowler, Thin filament length regulation in striated muscle sarcomeres: pointed-end dynamics go beyond a nebulin ruler, Semin. Cell Dev. Biol. 19 (2008) 511–519, https://doi.org/10.1016/j.semcdb.2008.08.009.
- [20] H. Gong, V. Hatch, L. Ali, W. Lehman, R. Craig, L.S. Tobacman, Mini-thin filaments regulated by troponin-tropomyosin, Proc. Natl. Acad. Sci. U. S. A 102 (2005) 656–661, https://doi.org/10.1073/pnas.0407225102.
- [21] D.S. Gokhin, V.M. Fowler, Tropomodulin capping of actin filaments in striated muscle development and physiology, J. Biomed. Biotechnol. 2011 (2011) 103069, https://doi.org/10.1155/2011/103069.
- [22] X. Chen, F. Ni, E. Kondrashkina, J. Ma, Q. Wang, Mechanisms of leiomodin 2-mediated regulation of actin filament in muscle cells, Proc. Natl. Acad. Sci. U. S. A 112 (2015) 12687–12692, https://doi.org/10.1073/pnas.1512464112.
- [23] D. Chereau, M. Boczkowska, A. Skwarek-Maruszewska, I. Fujiwara, D.B. Hayes, G. Rebowski, P. Lappalainen, T.D. Pollard, R. Dominguez, Leiomodin is an actin filament nucleator in muscle cells, Science 320 (2008) 239–243, https://doi.org/ 10.1126/science.1155313.

- [24] M. Boczkowska, G. Rebowski, E. Kremneva, P. Lappalainen, R. Dominguez, How Leiomodin and Tropomodulin use a common fold for different actin assembly functions, Nat. Commun. 6 (2015) 8314, https://doi.org/10.1038/ncomms9314.
- [25] D. Tolkatchev, G.E. Smith, L.E. Schultz, M. Colpan, G.L. Helms, J.R. Cort, C. C. Gregorio, A.S. Kostyukova, Leiomodin creates a leaky cap at the pointed end of actin-thin filaments, PLoS Biol. 18 (2020), e3000848, https://doi.org/10.1371/ JOURNAL_PBIO.3000848.
- [26] D.F. McKillop, M.A. Geeves, Regulation of the interaction between actin and myosin subfragment 1: evidence for three states of the thin filament, Biophys. J. 65 (1993) 693–701, https://doi.org/10.1016/S0006-3495(93)81110-X.
- [27] A.V. Hill, The heat of shortening and the dynamic constants of muscle, Proc. R. Soc. B Biol. Sci. 126 (1938) 136–195, https://doi.org/10.1098/rspb.1938.0050.
- [28] R.W. Lymn, E.W. Taylor, Mechanism of adenosine triphosphate hydrolysis by actomyosin, Biochemistry 10 (1971) 4617–4624, https://doi.org/10.1021/ bi00801a004
- [29] E. Eisenberg, T.L. Hill, Y. Chen, Cross-bridge model of muscle contraction. Quantitative analysis, Biophys. J. 29 (1980) 195–227, https://doi.org/10.1016/ S0006-3495(80)85126-5.
- [30] T.L. Hill, E. Eisenberg, L. Greene, Theoretical model for the cooperative equilibrium binding of myosin subfragment 1 to the actin-troponin-tropomyosin complex, Proc. Natl. Acad. Sci. U.S.A. 77 (1980) 3186–3190.
- [31] J.J. Rice, F. Wang, D.M. Bers, P.P. de Tombe, Approximate model of cooperative activation and crossbridge cycling in cardiac muscle using ordinary differential equations, Biophys. J. 95 (2008) 2368–2390, https://doi.org/10.1529/ biophysi.107.119487.
- [32] M.V. Razumova, A.E. Bukatina, K.B. Campbell, Different myofilament nearest-neighbor interactions have distinctive effects on contractile behavior, Biophys. J. 78 (2000) 3120–3137, https://doi.org/10.1016/S0006-3495(00)76849-4.
- [33] S.G. Campbell, F.V. Lionetti, K.S. Campbell, A.D. McCulloch, Coupling of adjacent tropomyosins enhances cross-bridge-mediated cooperative activation in a markov model of the cardiac thin filament, Biophys. J. 98 (2010) 2254–2264, https://doi. org/10.1016/j.bpj.2010.02.010.
- [34] T.L. Daniel, A.C. Trimble, P.B. Chase, Compliant realignment of binding sites in muscle: transient behavior and mechanical tuning, Biophys. J. 74 (1998) 1611–1621, https://doi.org/10.1016/S0006-3495(98)77875-0.
- [35] B.C.W. Tanner, T.L. Daniel, M. Regnier, Filament compliance influences cooperative activation of thin filaments and the dynamics of force production in skeletal muscle, PLoS Comput. Biol. 8 (2012), https://doi.org/10.1371/journal. pcbi.1002506.
- [36] S.M. Mijailovich, O. Kayser-Herold, B. Stojanovic, D. Nedic, T.C. Irving, M. A. Geeves, Three-dimensional stochastic model of actin-myosin binding in the sarcomere lattice, J. Gen. Physiol. 148 (2016) 459–488, https://doi.org/10.1085/jgp.201611608.
- [37] K.S. Campbell, Filament compliance effects can explain tension overshoots during force development, Biophys. J. 91 (2006) 4102–4109, https://doi.org/10.1529/ biophysj.106.087312.
- [38] P.B. Chase, J.M. Macpherson, T.L. Daniel, A spatially explicit nanomechanical model of the half- sarcomere: myofilament compliance affects Ca2+-Activation, Ann. Biomed. Eng. 32 (2004) 1559–1568.
- [39] C.D. Williams, M. Regnier, T.L. Daniel, J.M. Squire, F. Carreras-Costa, Elastic energy storage and radial forces in the myofilament lattice depend on sarcomere length, PLoS Comput. Biol. 8 (2012), e1002770, https://doi.org/10.1371/journal. pcbi 1002770
- [40] S. Land, S.A. Niederer, A spatially detailed model of isometric contraction based on competitive binding of troponin I explains cooperative interactions between tropomyosin and crossbridges, PLoS Comput. Biol. 11 (2015) 1–28, https://doi. org/10.1371/journal.pcbi.1004376.
- [41] B.C.W. Tanner, M. McNabb, B.M. Palmer, M.J. Toth, M.S. Miller, Random myosin loss along thick-filaments increases myosin attachment time and the proportion of bound myosin heads to mitigate force decline in skeletal muscle, Arch. Biochem. Biophys. 552–553 (2014) 117–127, https://doi.org/10.1016/j.abb.2014.01.015.
- [42] A.J. Fenwick, A.M. Wood, B.C.W. Tanner, Effects of cross-bridge compliance on the force-velocity relationship and muscle power output, PloS One 12 (2017), e0190335, https://doi.org/10.1371/journal.pone.0190335.
- [43] S. Walcott, Muscle activation described with a differential equation model for large ensembles of locally coupled molecular motors, Phys. Rev. E - Stat. Nonlinear Soft Matter Phys. 90 (2014), 042717, https://doi.org/10.1103/PhysRevE.90.042717.
- [44] B.C.W. Tanner, T.L. Daniel, M. Regnier, Sarcomere lattice geometry influences cooperative myosin binding in muscle, PLoS Comput. Biol. 3 (2007), e115, https://doi.org/10.1371/journal.pcbi.0030115.
- [45] S.M. Mijailovich, O. Kayser-Herold, B. Stojanovic, D. Nedic, T.C. Irving, M. A. Geeves, Three-dimensional stochastic model of actin-myosin binding in the sarcomere lattice, J. Gen. Physiol. 148 (2016) 459–488, https://doi.org/10.1085/ipn.2016.11608
- [46] S.M. Mijailovich, B. Stojanovic, D. Nedic, M. Svicevic, M.A. Geeves, T.C. Irving, H. L. Granzier, Nebulin and titin modulate cross-bridge cycling and length-dependent calcium sensitivity, J. Gen. Physiol. 151 (2019) 680–704, https://doi.org/10.1085/jgp.201812165.
- [47] C.D. Williams, M. Regnier, T.L. Daniel, Elastic energy storage and radial forces in the myofilament lattice depend on sarcomere length, PLoS Comput. Biol. 8 (2012), e1002770, https://doi.org/10.1371/journal.pcbi.1002770.
- [48] C. David Williams, M. Regnier, T.L. Daniel, Axial and radial forces of cross-bridges depend on lattice spacing, PLoS Comput. Biol. 6 (2010), https://doi.org/10.1371/ journal.pcbi.1001018.
- [49] L. Marcucci, T. Washio, T. Yanagida, Titin-mediated thick filament activation, through a mechanosensing mechanism, introduces sarcomere-length dependencies

- in mathematical models of rat trabecula and whole ventricle, Sci. Rep. 7 (2017), https://doi.org/10.1038/s41598-017-05999-2.
- [50] J. Howard, Mechanics of Motor Proteins and the Cytoskeleton, Sinauer Associates, Publishers. 2001.
- [51] M. Linari, M. Caremani, C. Piperio, P.W. Brandt, V. Lombardi, Stiffness and fraction of Myosin motors responsible for active force in permeabilized muscle fibers from rabbit psoas, Biophys. J. 92 (2007) 2476–2490, https://doi.org/10.1529/ biophysj.106.099549.
- [52] G. Piazzesi, L. Lucii, V. Lombardi, The size and the speed of the working stroke of muscle myosin and its dependence on the force, J. Physiol. 545 (2002) 145–151, https://doi.org/10.1113/jphysiol.2002.028969.
- [53] A.M. Gordon, A.F. Huxley, F.J. Jitliant, F.J. Julian, The variation in isometric tension with sarcomere length in vertebrate muscle fibers, J. Physiol. 184 (1966) 170–192.
- [54] M. Regnier, A.J. Rivera, C.-K.K. Wang, M.A. Bates, P.B. Chase, A.M. Gordon, Thin filament near-neighbour regulatory unit interactions affect rabbit skeletal muscle steady-state force-Ca2+ relations, J. Physiol. 540 (2002) 485–497, https://doi.org/ 10.1113/jphysiol.2001.013179.
- [55] T.E. Gillis, D.A. Martyn, A.J. Rivera, M. Regnier, Investigation of thin filament near-neighbour regulatory unit interactions during force development in skinned cardiac and skeletal muscle, J. Physiol. 580 (2007) 561–576, https://doi.org/ 10.1113/jphysiol.2007.128975.
- [56] D.M. Bers, Cardiac excitation-contraction coupling, Nature 415 (2002) 198–205, https://doi.org/10.1038/415198a.
- [57] F. Li, D. Buck, J.M. De Winter, J. Kolb, H. Meng, C. Birch, R. Slater, Y.N. Escobar, J. E. Smith, L. Yang, J. Konhilas, M.W. Lawlor, C.A.C. Ottenheijm, H.L. Granzier, Nebulin deficiency in adult muscle causes sarcomere defects and muscle-type-dependent changes in trophicity: novel insights in nemaline myopathy, Hum. Mol. Genet. 24 (2015) 5219–5233, https://doi.org/10.1093/hmg/ddv243.
- [58] C.A.C. Ottenheijm, P. Hooijman, E.T. DeChene, G.J.M. Stienen, A.H. Beggs, H. L. Granzier, Altered myofilament function depresses force generation in patients with nebulin-based nemaline myopathy (NEM2), J. Struct. Biol. 170 (2010) 334–343, https://doi.org/10.1016/j.jsb.2009.11.013.
- [59] S.G. Page, H.E. Huxley, Filament lengths in striated muscle, J. Cell Biol. 19 (1963) 369–390, https://doi.org/10.1083/jcb.19.2.369.
- [60] K. Trombitás, L. Frey, G.H. Pollack, Filament lengths in frog semitendinosus and tibialis anterior muscle fibres, J. Muscle Res. Cell Motil. 14 (1993) 167–172, https://doi.org/10.1007/BF00115451.
- [61] R. Littlefield, V.M. Fowler, Measurement of thin filament lengths by distributed deconvolution analysis of fluorescence images, Biophys. J. 82 (2002) 2548, https://doi.org/10.1016/S0006-3495(02)75598-7.
- [62] H.L.M. Granzier, H.A. Akster, H.E.D.J. Ter Keurs, Effect of thin filament length on the force-sarcomere length relation of skeletal muscle, Am. J. Physiol. Cell Physiol. 260 (1991), https://doi.org/10.1152/ajpcell.1991.260.5.c1060.
- [63] T.J. Burkholder, R.L. Lieber, Sarcomere length operating range of vertebrate muscles during movement, J. Exp. Biol. 204 (2001) 1529–1536.
- [64] T.F. Robinson, S. Winegrad, The measurement and dynamic implications of thin filament lengths in heart muscle, J. Physiol. 286 (1979) 607–619, https://doi.org/ 10.1113/jphysiol.1979.sp012640.
- [65] M.-L.L. Bang, X. Li, R. Littlefield, S. Bremner, A. Thor, K.U. Knowlton, R.L. Lieber, J. Chen, Nebulin-deficient mice exhibit shorter thin filament lengths and reduced contractile function in skeletal muscle, J. Cell Biol. 173 (2006) 905–916, https://doi.org/10.1083/icb.200603119
- [66] D.S. Gokhin, M.-L.L. Bang, J. Zhang, J. Chen, R.L. Lieber, Reduced thin filament length in nebulin-knockout skeletal muscle alters isometric contractile properties, Am. J. Physiol. Cell Physiol. 296 (2009) C1123–C1132, https://doi.org/10.1152/ aived1.00503.2008
- [67] K. Pelin, P. Hilpelä, K. Donner, C.A. Sewry, P.a. Akkari, S.D. Wilton, D. Wattanasirichaigoon, M.-L.L. Bang, T. Centner, F. Hanefeld, S. Odent, M. Fardeau, J.A. Urtizberea, F. Muntoni, V. Dubowitz, A.H. Beggs, N.G. Laing, S. Labeit, A. de la Chapelle, C. Wallgren-Pettersson, Mutations in the nebulin gene associated with autosomal recessive nemaline myopathy, Proc. Natl. Acad. Sci. U. S. A 96 (1999) 2305–2310. https://doi.org/10.1073/pngs.96.5.2305
- S. A 96 (1999) 2305–2310, https://doi.org/10.1073/pnas.96.5.2305.
 M. Chandra, R. Mamidi, S. Ford, C. Hidalgo, C. Witt, C.A.C. Ottenheijm, S. Labeit, H.L. Granzier, R. Manidi, Nebulin alters cross-bridge cycling kinetics and increases thin filament activation. A novel mechanism for increasing tension and reducing tension cost, J. Biol. Chem. 284 (2009) 30889–30896, https://doi.org/10.1074/jbs/M100.040718
- [69] M.-L.L. Bang, M. Caremani, E. Brunello, R. Littlefield, R.L. Lieber, J. Chen, V. Lombardi, M. Linari, Nebulin plays a direct role in promoting strong actinmyosin interactions, Faseb. J. 23 (2009) 4117–4125, https://doi.org/10.1096/ fi.09-137729.
- [70] D.G. Stephenson, D.A. Williams, Effects of sarcomere length on the force-pCa relation in fast- and slow-twitch skinned muscle fibres from the rat, J. Physiol. 333 (1982) 637–653.
- [71] R. Horowits, R.J. Podolsky, R. Horrowits, R.J. Podolsky, The positional stability of thick filaments in activated skeletal muscle depends on sarcomere length: evidence for the role of titin filaments, J. Cell Biol. 105 (1987) 2217–2223, https://doi.org/ 10.1083/jcb.105.5.2217.
- [72] N. Fukuda, Y. Wu, G.P. Farman, T.C. Irving, H.L. Granzier, Titin isoform variance and length dependence of activation in skinned bovine cardiac muscle, J. Physiol. 553 (2003) 147–154, https://doi.org/10.1113/jphysiol.2003.049759.

- [73] W.A. Linke, Sense and stretchability: the role of titin and titin-associated proteins in myocardial stress-sensing and mechanical dysfunction, Cardiovasc. Res. 77 (2008) 637–648, https://doi.org/10.1016/j.cardiores.2007.03.029.
- [74] M. Linari, E. Brunello, M. Reconditi, L. Fusi, M. Caremani, T. Narayanan, G. Piazzesi, V. Lombardi, M. Irving, Force generation by skeletal muscle is controlled by mechanosensing in myosin filaments, Nature 528 (2015) 276–279, https://doi.org/10.1038/nature15727.
- [75] J.D. Allen, R.L. Moss, Factors influencing the ascending limb of the sarcomere length-tension relationship in rabbit skinned muscle fibres, J. Physiol. 390 (1987) 119–136, https://doi.org/10.1113/jphysiol.1987.sp016689.
- [76] J.P. Konhilas, T.C. Irving, P.P. de Tombe, Length-dependent activation in three striated muscle types of the rat, J. Physiol. 544 (2002) 225–236, https://doi.org/ 10.1113/jphysiol.2002.024505.
- [77] H.E. ter Keurs, T. Iwazumi, G.H. Pollack, The sarcomere length-tension relation in skeletal muscle, J. Gen. Physiol. 72 (1978) 565–592, https://doi.org/10.1085/ ion.72.4.565.
- [78] G.P. Farman, D.B. Gore, E. Allen, K. Schoenfelt, T.C. Irving, P.P. de Tombe, Myosin head orientation: a structural determinant for the Frank-Starling relationship, Am. J. Physiol. Heart Circ. Physiol. 300 (2011) H2155–H2160, https://doi.org/ 10.1152/ajpheart.01221.2010.
- [79] T.C. Irving, Y. Wu, T. Bekyarova, G.P. Farman, N. Fukuda, H.L. Granzier, Thick-filament strain and interfilament spacing in passive muscle: effect of titin-based passive tension, Biophys. J. 100 (2011) 1499–1508, https://doi.org/10.1016/j.bpj.2011.01.059.
- [80] O. Cazorla, Y. Wu, T.C. Irving, H.L. Granzier, Titin-based modulation of calcium sensitivity of active tension in mouse skinned cardiac myocytes, Circ. Res. 88 (2001) 1028–1035.
- [81] C.A.C. Ottenheijm, H.W.H. van Hees, L.M.A. Heunks, H.L. Granzier, Titin-based mechanosensing and signaling: role in diaphragm atrophy during unloading? Am. J. Physiol. Lung Cell Mol. Physiol. 300 (2011) L161–L166, https://doi.org/ 10.1152/ajplung.00288.2010.
- [82] K.C. Nishikawa, J.A. Monroy, T.E. Uyeno, S.H. Yeo, D.K. Pai, S.L. Lindstedt, Is titin a "winding filament"? A new twist on muscle contraction, Proc. R. Soc. B Biol. Sci. 279 (2012) 981–990, https://doi.org/10.1098/rspb.2011.1304.
- [83] C. Rode, T. Siebert, R. Blickhan, Titin-induced force enhancement and force depression: a "sticky-spring" mechanism in muscle contractions? J. Theor. Biol. 259 (2009) 350–360, https://doi.org/10.1016/j.jtbi.2009.03.015.
- [84] A. Moreno-Gonzalez, T.E. Gillis, A.J. Rivera, P.B. Chase, D.A. Martyn, M. Regnier, Thin-filament regulation of force redevelopment kinetics in rabbit skeletal muscle fibres, J. Physiol. 579 (2007) 313–326, https://doi.org/10.1113/ iphysiol.2006.124164.
- [85] C.A. Morris, L.S. Tobacman, E. Homsher, Modulation of contractile activation in skeletal muscle by a calcium-insensitive troponin C mutant, J. Biol. Chem. 276 (2001) 20245–20251, https://doi.org/10.1074/jbc.M007371200.
- [86] J.M. Metzger, R.L. Moss, Kinetics of a Ca2+-sensitive cross-bridge state transition in skeletal muscle fibers: effects due to variations in thin filament activation by extraction of troponin C, J. Gen. Physiol. 98 (1991) 233–248, https://doi.org/ 10.1085/jgp.98.2.233.
- [87] K.B. Campbell, Rate constant of muscle force redevelopment reflects cooperative activation as well as cross-bridge kinetics, Biophys. J. 72 (1997) 254–262, https://doi.org/10.1016/S0006-3495(97)78664-8.
- [88] L.S. Tobacman, Thin filament-mediated regulation of cardiac contraction, Annu. Rev. Physiol. 58 (1996) 447–481, https://doi.org/10.1146/annurev. ph 58 030196 002311
- [89] R.J. Solaro, H.M. Rarick, Troponin and tropomyosin: proteins that switch on and tune in the activity of cardiac myofilaments, Circ. Res. 83 (1998) 471–480, https://doi.org/10.1161/01.RES.83.5.471.
- [90] L.R. Nyland, B.M. Palmer, Z. Chen, D.W. Maughan, C.E. Seidman, J.G. Seidman, L. Kreplak, J.O. Vigoreaux, Cardiac myosin binding protein-C is essential for thickfilament stability and flexural rigidity, Biophys. J. 96 (2009) 3273–3280, https:// doi.org/10.1016/j.bpj.2008.12.3946.
- [91] M.J. Previs, B.L. Prosser, J.Y. Mun, S.B. Previs, J. Gulick, K. Lee, J. Robbins, R. Craig, W.J. Lederer, D.M. Warshaw, Myosin-binding protein C corrects an intrinsic inhomogeneity in cardiac excitation-contraction coupling, Sci. Adv. 1 (2015), 1400205, https://doi.org/10.1126/sciadv.1400205.
- [92] J.E. Stelzer, D.P. Fitzsimons, R.L. Moss, Ablation of myosin-binding protein-C accelerates force development in mouse myocardium, Biophys. J. 90 (2006) 4119–4127, https://doi.org/10.1529/biophysj.105.078147.
- [93] M. Reconditi, M. Linari, L. Lucii, A. Stewart, A. Stawart, Y.-B.B. Sun, P. Beesecke, T. Narayanan, R.F. Fischetti, T.C. Irving, G. Piazzesi, M. Irving, V. Lombardi, The myosin motor in muscle generates a smaller and slower working stroke at higher load, Nature 428 (2004) 578–581, https://doi.org/10.1038/nature02380.
- [94] J.W.S. Pringle, Stretch activation of muscle: function and mechanism, Proc. R. Soc. London Biol. Sci. 201 (1978) 107–130, https://doi.org/10.1098/rspb.1978.0035.
 [95] D. Labeit, K. Watanabe, C. Witt, H. Fujita, Y. Wu, S. Lahmers, T. Funck, S. Labeit,
- [95] D. Labett, K. Watanabe, C. Witt, H. Fujita, Y. Wu, S. Lahmers, T. Funck, S. Laber H. Granzier, Calcium-dependent molecular spring elements in the giant protein titin, Proc. Natl. Acad. Sci. U. S. A 100 (2003) 13716–13721, https://doi.org/ 10.1073/pnas.2235652100.
- [96] K. Nishikawa, S. Dutta, M. DuVall, B. Nelson, M.J. Gage, J.A. Monroy, Calcium-dependent titin-thin filament interactions in muscle: observations and theory, J. Muscle Res. Cell Motil. 41 (2020) 125–139, https://doi.org/10.1007/s10974-019-09540-v.